Journal of Ceramic Processing Research. Vol. 24, No. 6, pp. 963~967 (2023)
(Received 16 August 2023, Received in revised form 18 October 2023, Accepted 28 October 2023)
https://doi.org/10.36410/jcpr.2023.24.6.963

J O U R N A L O F
Ceramic Processing Research

Synthesis of $Ca_{14}Zn_6Al_{10}O_{35}:Mn^{4+}$, Nd^{3+} phosphor using starch as an impregnation medium

Soo-Jong Kim*
Department of Chemical Engineering, Halla University, 28 Halladaegil, Wonju, Gangwon State, 26404, Korea

$Ca_{14}Zn_6Al_{10}O_{35}:Mn^{4+}$, Nd^{3+} phosphors were prepared by a liquid phase impregnation method. The results of XRD, SEM, and EDS analysis confirmed that pure CZA:Mn^{4+} and CZA:Mn^{4+}, Nd^{3+} phosphors with single phases were synthesized. The Mn^{4+} doped phosphors exhibited strong red emission in the range of 600 to 850 nm when excited at a wavelength of 356 nm. The luminescence properties were investigated according to changes in the concentrations of Mn^{4+} and Nd^{3+} ions. The particle sizes of the phosphor when fired at 1200 °C for 3 hours were 100 to 500 nm.

Keywords: $Ca_{14}Zn_6Al_{10}O_{35}$: Mn^{4+}, Nd^{3+}, Starch, Red phosphor.

Introduction

Changes in the Earth's climate have become more serious in recent years. However, these changes in climate can be offset by growing eco-friendly crops in plant factories. Plant factories are operating in several places. In plant factories, LEDs with phosphors as key components are usually utilized [1-3]. Most phosphor materials emitting multiple wavelengths are manufactured in a reducing atmosphere [4]. However, this study aimed to develop $Ca_{14}Zn_6Al_{10}O_{35}:Mn^{4+}$, Nd^{3+} red fluorescent materials that can be easily manufactured in air. The wavelength emitted by $Ca_{14}Zn_6Al_{10}O_{35}:Mn^{4+}$ red phosphor is 660 nm, and its irradiation to plants increases the efficiency of photosynthesis, which greatly promotes plant growth [5, 6]. To synthesize phosphor particles, various liquid synthesis methods such as sol-gel method, hydrothermal synthesis method, microemulsion method, and precipitation method have been attempted [7-11]. In this synthesis method, a precursor precipitation process is essentially applied. This precipitation operation uses a large amount of solvent, and metal hydroxide precipitate is obtained in the form of metal hydroxide salt. Since metal oxide nanoparticles are manufactured through filtration, dehydration, and heat treatment of precipitated metal hydroxide, a large amount of waste solvent generated during this process must be recovered or treated, and the cost incurred at this time becomes a problem [12]. Therefore, the most important point in these various liquid synthesis methods is to reduce manufacturing costs by using a method that is simple in the process and does not generate waste water solutions. In this study, $Ca_{14}Zn_6Al_{10}O_{35}:Mn^{4+}$, Nd^{3+} phosphor precursors were prepared by impregnating starch, which is a natural polymer with a microfibril structure, with an aqueous solution of metal salts such as Ca, Zn, Al, Mn, and Eu. This precursor was dried and calcined to synthesize phosphor particles. Since the shape of the generated $Ca_{14}Zn_6Al_{10}O_{35}:Mn^{4+}$, Nd^{3+} phosphor particles is determined by the microstructure of starch, the crystal shape and particle size can be controlled [13]. This synthesis method does not involve using large amounts of solvents, such as precipitation processes, nor does it involve alkaline aqueous solutions. In addition, phosphors can be manufactured at firing temperatures lower than the solid phase method [14, 15]. Therefore, there is no need for solvent recovery or treatment, and it is possible to obtain uniform phosphor particles at a relatively low temperature [16]. By synthesis method used in this study is heat treated by impregnating a hydrate of a metal salt or metal salt in a polymer matrix to produce the ceramic fine particles, it is possible to easily manufacture the ceramic multi-component particles [17]. The starch, pulp and crystalline cellulose used as a cellulose source in the impregnation operation and there are microfibrillar structure and molecular fine structure of a size below few hundreds nm. In the impregnation process, metal salt aqueous solution ions enter and settle in an empty space between these molecular chains. Therefore, the shape of the particles produced after the heat treatment is a powder which particle size is uniform, depending on the microstructure of the starch, pulp etc. This synthesis method can easily control the particle size from different types of the matrices such as starch, pulp and crystalline cellulose, or by changing the firing conditions [18]. And it has the advantage that you do not use strong alkaline

*Corresponding author:
Tel : +82-33-760-1237
Fax: +82-33-760-1290
E-mail: sjkim@halla.ac.kr

organic solvents used in other synthesis methods, such as co-precipitation method. $Ca_{14}Zn_6Al_{10}O_{35}:Mn^{4+}$, Nd^{3+} phosphors can generate wavelengths of 650 to 770 nm and emit far-infrared rays that can match the absorption spectrum of plant pigments, so they are applied to indoor plant cultivation [19, 20]. $Ca_{14}Zn_6Al_{10}O_{35}$: Mn^{3+}, Nd^{3+} phosphors produced by the synthesis method used in this study emit wavelengths similar to those of sunlight. Therefore, they can provide an environment suitable for plant growth.

Experimental

The samples were prepared by the liquid phase impregnation method. The raw materials were $Ca(NO_3)_2{\cdot}4H_2O$, $Mn(NO_3)_2{\cdot}6H_2O$, $Al_2(NO_3)_3{\cdot}9H_2O$, $Zn(NO_3)_2{\cdot}6H_2O$ and $Nd(NO_3)_3{\cdot}6H_2O$. All reagents were analytically pure and used without further purification. Nitrates were used as metal salt starting materials, and aqueous solutions were prepared to have a predetermined concentration. The % concentration of the aqueous solutions of $Al_2(NO_3)_3{\cdot}9H_2O$ and $Mn(NO_3)_2{\cdot}6H_2O$ was 15%, $Ca(NO_3)_2{\cdot}4H_2O$ and $Zn(NO_3)_2{\cdot}6H_2O$ was 20%, and $Nd(NO_3)_3{\cdot}6H_2O$ was 2.25%. All the solutions were added to beakers and mixed for 2 hours while stirring with a magnetic stirrer. Then each mixed aqueous solution was poured into starch powder. The starch and each precursor solution were impregnated at a weight ratio of 1:1.3. After standing for 2 h, the impregnated mixtures were dried at 120 °C for 3 hours to obtain precursors. The dried precursors were calcined in an electric furnace at 500 °C for 1 hour to remove the organic components in the precursor and the starch. The calcined samples were pulverized with agate and then calcined in an electric furnace at a temperature range of 600 °C to 1,200 °C (heating rate: 5 °C/min) for 1 to 3 hours. The calcined samples were pulverized to obtain the final $Ca_{14}Zn_6Al_{10}O_{35}$: Mn^{3+}, Nd^{3+} powder. The x-ray diffraction pattern was investigated using the PANalytical X'Pert Pro X-ray diffractometer at UC Davis. Cu-Kα with a Ni filter was used to measure at a scanning speed of 5°/min, an acceleration voltage of 40 kV, and an acceleration current of 30 mA at a diffraction angle (2θ) range of 10 to 80°. FE-SEM (JEOL:JSM-7610F) was used to analyze the surface structure of the prepared $Ca_{14}Zn_6Al_{10}O_{35}$: Mn^{3+}, Nd^{3+} powder.

Results and Discussion

The crystal structure of $Ca_{14}Zn_6Al_{10}O_{35}$ is a cubic symmetrical lattice structure, a = 1.4868 nm, and the spatial group is F23 [21]. Fig. 1 shows the XRD patterns of the $Ca_{14}Zn_6Al_{10}O_{35}$:Mn samples obtained by firing at 1,000 °C and 1,200 °C for 3 hours. The XRD pattern is shown according to the change in concentration (0.03, 0.05, 0.07, and 0.1 mol%) of the Mn ions used as an activator. It has been reported that $Ca_{14}Zn_6Al_{10}O_{35}$ synthesized by the solid phase method has calcium oxide (CaO) as an impurity [19]. However, it can be seen from the XRD pattern that pure $Ca_{14}Zn_6Al_{10}O_{35}$ without calcium oxide was synthesized using the liquid precursor method in this study. All diffraction peaks coincide with the pattern of $Ca_{14}Zn_6Al_{10}O_{35}$ (JCPDS 50-0426), and there is no change in the crystal structure according to the concentration change of Mn [22]. In general, the phase purity of both the host lattice and the activated ion affects the emission characteristics of the phosphor. Mn^{4+} affects optical absorption behavior, and CZA host lattice affects both the chemical stability and optical properties of the phosphor. CZA:Mn^{4+} and CZA:Mn^{4+}, Nd^{3+} phosphors can be used as phosphors emitting wavelengths in the red region in LED lighting for plant factories. Since the wavelength in the 650-

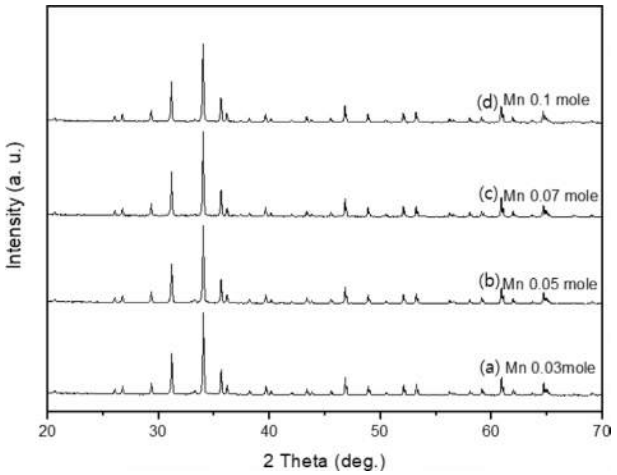

Fig. 1. XRD patterns of $Ca_{14}Zn_6Al_{9.92}O_{35}:Mn_{0.07}{}^{3+}$ phosphors with various Mn content, (a) 0.03 mole, (b) 0.05 mole, (c) 0.07 mole, and (d) 0.1 mole.

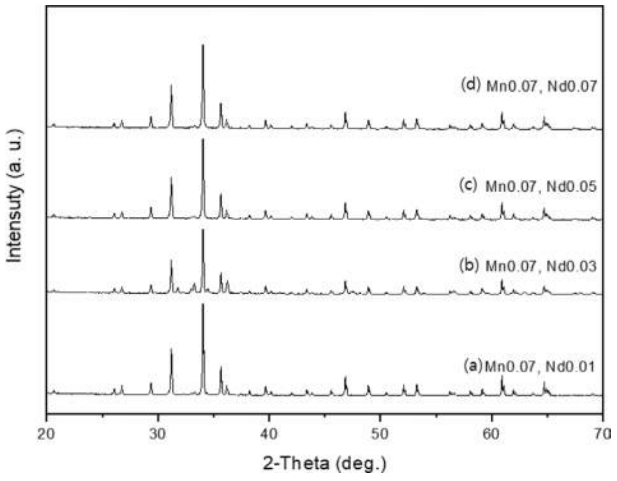

Fig. 2. XRD patterns of $Ca_{14}Zn_6Al_{9.92}O_{35}:Mn_{0.07}{}^{3+}$, $Nd_{0.01}{}^{3+}$ phosphor powders with various Nd content, (a) 0.03 mole, (b) 0.05 mole, (c) 0.07 mole, and (d) 0.1 mole, Mn was fixed 0.07 mole for each case.

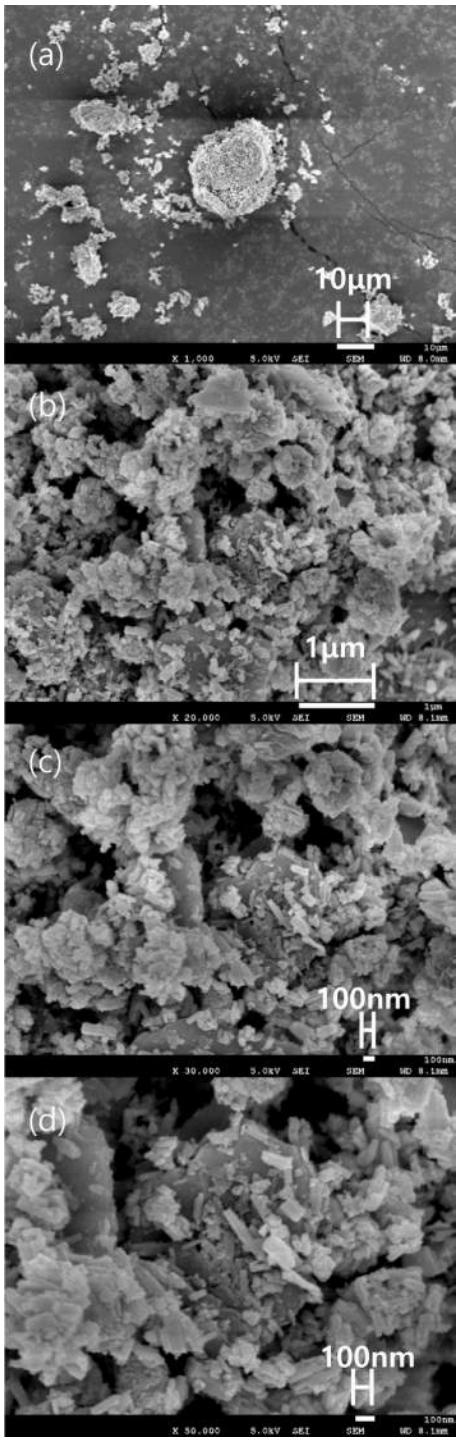

Fig. 3. SEM photograph of a $Ca_{14}Zn_6Al_{9.93}O_{35}$: $Mn_{0.07}^{3+}$, $Nd_{0.07}^{3+}$ phosphor fired at 1200 °C for 3 hours, multiplied by each (a)1,000, (b) 20,000, (c) 30,000, and (d) 50,000.

750 nm region emitted by CZA:Mn^{4+} and CZA:Mn^{4+}, Nd^{3+} phosphors is close to the maximum absorption wavelength of chlorophyll, the main photoreceptive pigment of plants, it is efficiently absorbed by plants to promote photosynthesis. Fig. 2 shows each XRD pattern according to the change in concentration (0.03, 0.05, 0.07, and 0.1 mol%) of Nd, a co-activator, while the Mn concentration is fixed at 0.07 mol. No changes in the diffraction peaks were observed according to the change in the concentration of Nd. Fig. 3 shows SEM photographs according to the change in the amount of Mn and Nd added. It was found that the change in the mol ratio of Mn and Nd did not affect the shape or size of the particles. Fig. 4 shows the EDS spectrum, electron image, and element analysis results of the $Ca_{14}Zn_6Al_{9.86}O_{35}:Mn_{0.07}^{4+}$, $Nd_{0.07}^{3+}$ samples fired at 1,200 °C for 3 hours. In the electron image, nanometer-sized phosphor particles in the form of flakes were observed. In the EDS spectrum, peaks of all elements constituting the phosphor compound were observed. Peaks specifying a sharp and strong intensity of Zn, Al, Ca, and O atoms and peaks of Mn and Nd were also observed, indicating that pure $Ca_{14}Zn_6Al_{9.86}O_{35}:Mn_{0.07}^{4+}$, $Nd_{0.07}^{3+}$ nanoparticles were generated. When used in optical devices such as LEDs, the uniformity of particle size and shape of the phosphor affects the optical properties [23, 24]. In the case of YAG:Ce phosphor, it was reported that the more uniform the particle size and shape, the higher the brightness. And particle size plays an important role in the packaging performance of phosphor-converted white LEDs [25]. The weight ratio of the phosphor particle components was 11.27 wt% of Ca, 34.72 wt% of O, 6.48 wt% of Al, and 30.9 wt% of Zn. In EDS analysis, if C is about 5.0%, the sample is considered to not contain carbon at all. In the EDS analysis, C was usually about 15%. Fig. 5 shows the results of the photoluminescence (PL) measurement of the $Ca_{14}Zn_6Al_{10}O_{35}:Mn^{4+}$, Nd^{3+} powder fired at 1,200 °C. The powder was excited with an Xe discharge lamp. The Mn^{4+} ion used as an activator serves as a luminescent center, and the Nd^{3-} ion used as a co-activator serves to compensate for the charge of the Mn^{4+} ion. Among the phosphors used as LED light sources in plant factories, $ZnGa_2O_4$:$0.02Cr^{3+}$ has been reported to emit wavelengths in the 650-750 nm range [26]. Phosphors that emit wavelengths in the 650-750 nm range have a significant effect on the chlorophyll of plants and promote growth [27]. The excitation spectrum of $Ca_{14}Zn_6Al_{10}O_{35}:Mn^{4+}$, Nd^{3+} was obtained by fixing the emission wavelength at 712 nm, and the emission spectrum was measured by fixing the excitation wavelength at 356 nm. Both red emission from Mn^{4+} and near infrared (NIR) emission from Nd^{3+} were observed from the $Ca_{14}Zn_6Al_{10}O_{35}:Mn^{4+}$, Nd^{3+} phosphors. The emission spectrum of $Ca_{14}Zn_6Al_{10}O_{35}:Mn^{4+}$, Nd^{3+} appeared in a wavelength range between 600 and 850 nm, and the maximum emission peak was 712 nm. Mn^{4+} ions are excited into their charge transfer or $^4T_1$, $^4T_2$ states by light irradiation. The excited Mn^{4+} ions rapidly relax to the ^2E state in the metastable state. In addition, energy transfer occurs for Mn^{4+} ions from the ^2E state to $^4A_2$ (698-712 nm), and for Nd^{3+} ions, energy transfer occurs from the $^4I_{9/2}$ state to $^4F_{9/2}$, $^4F_{7/2}$, and $^4S_{3/2}$, respectively [28-30]. Spin-forbidden

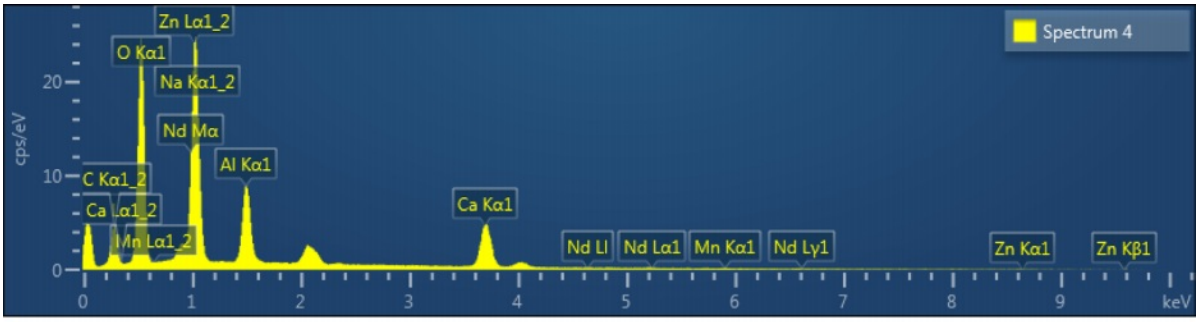

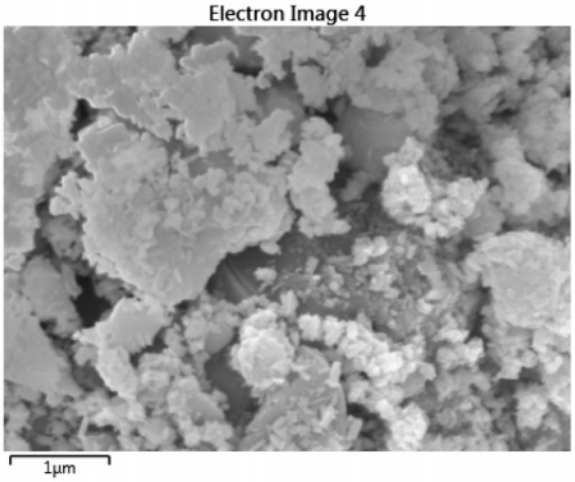

Element	Wt%	Wt% Sigma
C	13.55	0.29
O	34.72	0.3
Na	1.74	0.19
Al	6.48	0.09
Ca	11.27	0.15
Mn	0.39	0.23
Zn	30.9	0.31
Nd	0.96	0.4
Total:	100	

Fig. 4. EDS spectrum, SEM image and atomic Wt% of prepared $Ca_{14}Zn_6Al_{9.93}O_{35}:Mn_{0.07}^{3+}$, $Nd_{0.01}^{3+}$ phosphors at 1,200 °C.

transitions are transitions that occur in the triplet state. Spin-forbidden transitions emit light of lower energy than the wavelength of light emitted by spin-allowed transitions. Excitation into the absorption band at 356 nm gives an intense broad red emission around 712 nm originating from the $^2E \rightarrow {}^4A_2$ spin-forbidden transition of Mn^{4+} ions in $Ca_{14}Zn_6Al_{10}O_{35}:Mn^{4+}$, Nd^{3+} phosphors. The wavelength of light emitted from the spin-forbidden transition from the ^2E state to the $^4A_2$ state of the Mn ion in $Ca_{14}Zn_6Al_{10}O_{35}:Mn^{4+}$, Nd^{3+} phosphors is 650-750 nm. $Ca_{14}Zn_6Al_{10}O_{35}:Mn^{4+}$, Nd^{3+} phosphor have a spectral range of 650 to 750 nm that allows efficient cultivation of indoor plants, so they are applied to artificial lighting for plant factories.

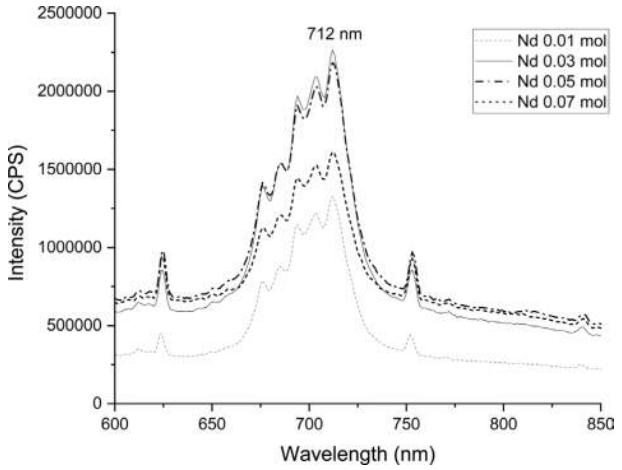

Fig. 4. EDS spectrum, SEM image and atomic Wt% of prepared $Ca_{14}Zn_6Al_{9.93}O_{35}:Mn_{0.07}^{3+}$, $Nd_{0.01}^{3+}$ phosphors at 1,200 ℃.

Conclusions

A precursor aqueous solution was prepared using Ca, Zn, Al, Mn, and Nd metal nitrates, with Mn and Nd as activators. This solution was used to synthesize a CZA:Mn^{4+}, Nd^{3+} phosphor by the liquid precursor method. Water-soluble starch $(C_6H_{10}O_5)_n$ was used as an impregnation medium. The surface structure, crystallinity, and luminescence characteristics of the synthesized CZA:Mn^{4+}, Nd^{3+} phosphor were analyzed. The results of the PL measurement showed that a deep red phosphor with an emission wavelength in the near-infrared region of 600 to 850 nm was successfully synthesized. The $Ca_{14}Al_{10}Zn_6O_{35}:Mn^{4+}$, Nd^{3+} phosphors can be excited by light irradiation and exhibit far-red emission due to the Mn^{4+} spin-forbidden ^2E to $^4A_2$ transition. The XRD analysis results confirmed that pure CZA:Mn^{4+} and CZA:Mn^{4+}, Nd^{3+} phosphor with a single phase were synthesized. The results of SEM and EDS analysis showed that the synthesized $Ca_{14}Zn_6Al_{9.93}O_{35}:Mn^{4+}_{0.07}$, $Nd^{3+}_{0.07}$ phosphor powder had a uniform particle size with flake-shaped particles ranging from 100 to 500 nm. It was also confirmed that Mn and Nd ions used as activators were present.

Acknowledgements

This work was supported by a research grant from 2023 Halla University.

References

1. S.R. Bhelave, A.R. Kadam, A.N. Yerpude, and S.J. Dhoble, Luminescence. 38[4] (2023) 279-388.
2. W. Lü, W. Lv, Q. Zhao, M. Jiao, B. Shao, and H. You, Inorg. Chem. 53[22] (2014) 11985-11990.
3. S. Fang, T. Lang, M. Cai, and T. Han, J. Alloys Compd. 902 (2022) 163825.
4. K. Mori, Y. Kojima, and N. Nishimiya, Funct. Mater. Lett. 5[2] (2012) 1260012.
5. Z. Liu, G. Shao, W. Chen, G. Hu, L. Shen, Y. Cheng, X. Liang, and W. Xiang, Opt. Mater. Express. 8[9] (2018) 2532-2541.
6. Y. Zhong, S. Gai, M. Xia, S. Gu, Y. Zhang, X. Wu, J. Wang, N. Zhou, and Z. Zhou, Chem. Eng. J. 374 (2019) 381-391.
7. J. Lian, P. Liang, B. Wang, and F. Liu, J. Ceram. Process. Res. 15[6] (2014) 382-388.
8. H. Terraschke, M.F.T. Meier, Y. Voss, H. Schonherr, and C. Wickleder, J. Ceram. Process. Res. 16[1] (2015) 59-63.
9. X. Niu, J. Xu, Y. Zhang, Y. Chu, B. Yang, and C. Zhang, J. Ceram. Process. Res. 16[5] (2015) 609-613.
10. B.S. Kim, M.J. Lee, T. Abe, T. Masaki, Y.H. Song, K. Toda, and D.H. Yoon, J. Ceram. Process. Res. 17[4] (2016) 286-289.
11. Y.A. Roh, Y.H. song, T. Masaki, and D.H. Yoon, J. Ceram. Process. Res. 17[4] (2016) 300-303.
12. S.J. Kim and H.S. Kwon, J. Korean Inst. Electr. Electron. Mater. Eng. 20[8] (2007) 671-679.
13. Y.L. Song, S.H. Choi, S.J. Kim, Y.H. Song, T. Masaki, and D.H. Yoon, J. Ceram. Process. Res. 17[3] (2016) 202-204.
14. S.J. Kim and C.H. Han, J. Ceram. Process. Res. 19[2] (2018) 130-133.
15. G. Du, W. Guo, J.M.K. Al-zyadi, Y. Han, P. Liu, and Z. Liu, J. Nanopart. Res. 15 (2013) 1-8.
16. S.J. Kim, T. Masaki, S.H. Choi, and D.H. Yoon, J. Ceram. Process. Res. 17[4] (2016) 338-343.
17. S.J. Kim, J. Ceram. Process. Res. 22[1] (2021) 74-78.
18. S.J. Kim and C.H. Han, J. Ceram. Proc. Res. 19[2] (2018) 130-133.
19. N. Zhou, L. Liu, Z. Zhou, and Y. Zhang, J. Am. Ceram. Soc. 103[3] (2020) 1798-1808.
20. L. Li, H. Li, Z. Wu, G. Tian, Y. Wang, F. Ling, S. Jiang, G. Xiang, X. Zhou, and J. Xue, J. Lumin. 238 (2021) 118286.
21. K. Seki, K, Uematsu, K, Toda, and M. Sato, Chem. Lett. 43[8] (2014) 1213-1215.
22. T. Hasegawa, S.W. Kim, T. Abe, S. Kumagai, R. Yamanashi, K. Seki, K. Uematsu, K. Toda, and M. Sato, Chem. Lett. 45[9] (2016) 1096-1098.
23. W.N. Wang, W. Widiyastuti, T. Ogi, and W. Lenggoroe, Chem. Mater. 19[7] (2007) 1723-1730.
24. Y.J. Hua, H.P. Ma, C. Zhang, D.G. Deng, S.L. Zhao, L.H. Huang, et al. Chin. J. Lumin. 34[4] (2013) 427-432.
25. H.I. Won, H.H. Nersisyan, C.W. Won, and K.H. Lee, Mater. Chem. Phys. 129[3] (2011) 955-960.
26. C. Zhou, L. Peng, Z. Kong, M. Wu, M.S. Molokeev, Z. Zhou, J. Wang, and M. Xia, J. Mater. Chem. C 10 (2022) 5829-5839.
27. X. Kang, W. Yang, D. Ling, C. Jia, and W. Lü, Mater. Res. Bull. 140 (2021) 111301.
28. X. Gao, W. Xia, T. Chen, X. Yang, X. Jin, and S. Xiao, RSC Adv. 6 (2016) 7544-7552.
29. M.G. Hur, S.H. Choi, S.B. Kwon, T. Masaki, K. Toda, and D.H. Yoon, Ceram. Int. 44 (2018) 15868-15872.
30. Z. Liao, H. Xu, W. Zhao, H. Yang, J. Zhong, H. Zhang, Z. Ni, and Z.K. Zhou, Chem. Eng. J. 395 (2020) 125060.